Essential Readings in Light Metals: Electrode Technology for Aluminum Production.
Edited by Alan Tomsett and John Johnson.
© 2013 The Minerals, Metals & Materials Society. Published 2013 by John Wiley & Sons, Inc.
Light Metals — From *Light Metals 1992*, Euel R. Cutshall, Editor

SODIUM AND BATH PENETRATION INTO TiB_2-CARBON CATHODES DURING LABORATORY ALUMINIUM ELECTROLYSIS

Jilai Xue and Harald A. Øye
Institute of Inorganic Chemistry
7034 Trondheim, Norway

ABSTRACT

TiB_2-carbon cathodes with varying amount of TiB_2 were prepared by pressing and baking. The TiB_2 bonded strongly to the carbon matrix, the crushing strength being better than that of pure carbon. The shrinkage during baking was found to decrease with increasing amount of TiB_2. Penetration of sodium and bath was studied in a laboratory aluminium electrolysis set-up, the cathode being on top of the melt. The penetration velocity increased with increased TiB_2 content, current density and cryolite ratio, but reached a plateau at CR=3 or at 0.7 A/cm^2, respectively. The sodium concentration was lower in the TiB_2 area than that in the carbon matrix, and bath constituents were found on the TiB_2 grain boundaries. AlF_3 was depleted in the carbon area while NaF preferentially migrated to the TiB_2 area enhancing sodium generation and penetration.

INTRODUCTION

Most of the recent research and development on inert cathodes for use in aluminium reduction cells have been concentrated on the titanium diboride materials [1-10]. For evaluation of the performance and the service life of TiB_2 cathodes, it is important to estimate their chemical stability during aluminium electrolysis. The following factors should be taken into account:

1. Dissolution in molten cryolite and liquid aluminium.
2. Penetration of sodium, aluminium and bath.
3. Reactions on the surface and in the inner part of the cathodes.
4. Stress - corrosion within the cathode body.
5. Erosion at cathode surface.

It is believed that point 2 usually plays an important role in cathode deterioration. Some investigations have been made on point 1 by Finch [11], point 3 by Mazza et al. [12], and point 4 by Gesing and Wheeler [5], respectively. The mechanism of sodium and bath into pure carbon cathodes during aluminium electrolysis has also been studied by several authors [13-16].

In previous work, studies in the laboratory have been carried out on the dissolution of TiB_2 into liquid aluminium and the penetration of aluminium into TiB_2 cathodes [17]. The purpose of the present work is to gain an insight into the penetration process of sodium and bath into TiB_2-modifying carbon matrix cathodes, with characterization of their materials of interest for retrofit in existing cells.

EXPERIMENTAL

1. Preparation of Test Specimens

The test specimens of TiB_2-carbon cathode materials were made in the laboratory. The raw materials were electrocalcined anthracite from Eastalco, Koppers AMT 7320 binder and TiB_2 powder. The content of TiB_2 varied from 0 to 50 wt % with a constant amount of binder, as shown in Table 1. The specimens were about 70 mm long with a diameter of 15 mm, and were formed with a pressure up to 2 tons during 3 minutes. The green specimens were prebaked at about 150°C for 8 hours, then placed in a vessel packed with carbonaceous powders and heated to 1250°C during baking.

Table 1. Composition of TiB_2-carbon cathode specimens (wt%).

Type	TiB_2	Anthracite	Binder
T0	0	83	17
T20	20	63	17
T35	35	48	17
T50	50	33	17

2. Characterization

The apparent density of a cylindrical sample, green or baked, was calculated from the measured values of its dimensions and weight. The weight change during baking was also measured. The crushing strength was tested by a standard method for carbon materials [18], with the

requirement that the length to the diameter was equal to 2. In a quartz glass dilatometer [19], the thermal expansion /contraction during baking was determined under a nitrogen atmosphere, heating at 180°C/hour from ambient temperature to about 1000°C with the samples of 25 mm in diameter and 50 mm in length.

3. Penetration Experiment

The experiments were carried out in a reversed polarity apparatus shown in Figure 1. The test system was placed in a vertical tube furnace and held at 1000°C under a nitrogen atmosphere. A constant current was provided during electrolysis by means of a 6264B DC power supply. The cylindrical cathode specimen was immersed 2 mm into the cryolite melts and rotated at a speed of 180 r.p.m. After electrolysis, it was cut open along its axis from the unimmersed side. Then the penetration depth corresponding to a certain amount of sodium content (about 3 %) was measured by a phenolphthalein test [19].

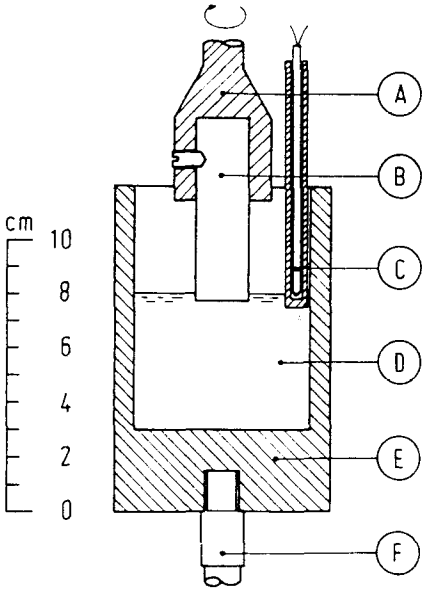

Figure 1. Reversed polarity apparatus. A) Graphite support, B) Test specimen (cathode), C) Thermocouple, D) Cryolite melt, E) Graphite crucible (anode), F) Graphite support rod.

4. Electron Microprobe Analysis

The samples were studied by backscatter electron image and electron image, using the JEOL superprobe 773. Simultaneously, x-ray emission mapping of titanium, sodium, aluminium and fluorine was carried out.

RESULTS AND DISCUSSION

1. Characterization of TiB_2-Carbon Cathode Materials

Some characteristic properties of the TiB_2-carbon cathode materials are given in Table 2. The density of samples, green or baked, increased as TiB_2 content increased due to the additive effect of TiB_2 with high density (about 4.4 g/cm^3) into the carbon matrix. In the range of 20% - 50% TiB_2 contents, the crushing strength of samples was better than that of pure carbon, but did not continue to increase with further increased TiB_2 content as expected.

Table 2. Some characteristic properties of TiB_2-carbon cathode materials.

Properties	T0	T20	T35	T50
Green density, g/cm^3	1.60	1.76	1.92	2.15
Apparent density, g/cm^3	1.35	1.69	1.86	2.07
Weight change during baking, %	-	+0.97	+5.03	+12.8
Crushing strength, MPa	14.4	47.0	18.9	-
Thermal expansion/ contraction #, %	-1.012	-0.540	-0.384	-

From 50°C - 1000°C - 50°C

Figure 2 shows that the total contraction of TiB_2-carbon cathode materials is less than that of pure carbon during baking, decreasing with increasing TiB_2 content, owing to the fact that the more stable TiB_2 particles occupies part of the bulk volume of the samples.

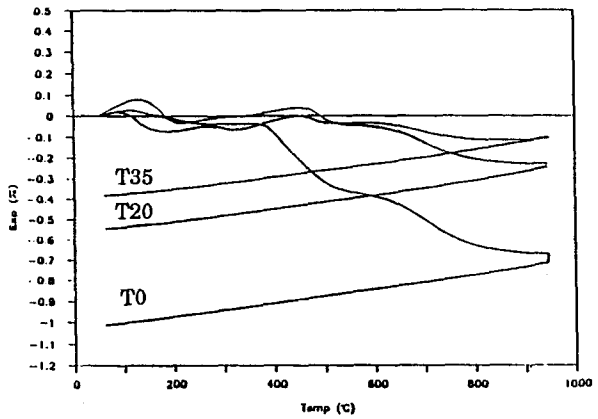

Figure 2. Thermal expansion/contraction of the samples. All samples were prebaked at 150°C before tests.

It was found that the present baking procedure protecting the samples by carbonaceous powders led to weight increase of the sample due to oxidation of TiB_2:

$$TiB_2 + 5/2\ O_2 = TiO_2 + B_2O_3 \qquad (1)$$

Some oxidation of the carbon components may also have occurred:

$$C + O_2 \rightarrow CO,\ CO_2 \qquad (2)$$

The weight increase was slight for the material with 20%

TiB_2, but unacceptably high for the sample with 50% TiB_2, where at least 22% of the TiB_2 was oxidized.

2. Effect of Cryolite Ratio and Current Density on Sodium Penetration

During aluminium electrolysis in cryolite melts, the sodium is mainly generated by a chemical reaction:

$$3\ NaF\ (l) + Al\ (l) = AlF_3\ (l) + 3\ Na\ (in\ C) \quad (3)$$

According to Equation (3), the sodium activity at the cathode surface is determined by the cryolite ratio for the melt in contact with the cathode. The surface sodium activity again provides the driving force for penetration of sodium into the cathode material. Figure 3 shows the penetration depth of sodium after electrolyzing for 4 hours with varied cryolite ratio. The penetration depth increased with CR and reached a plateau for CR = 3. This behaviour is very close to what was previously observed by Sørlie and Øye [16] for pure carbon cathodes.

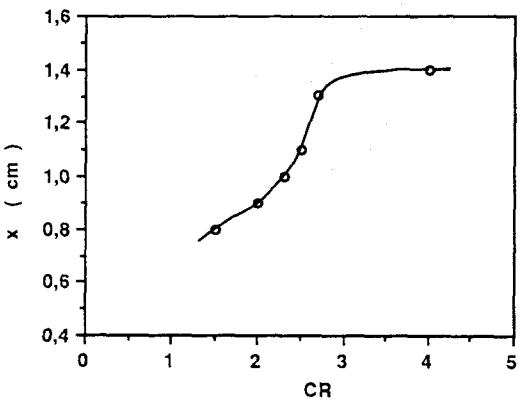

Figure 3. Plot of the sodium penetration depth versus the cryolite ratio of bath. T35 samples, CD = 0.5 A/cm^2, 1000°C, 4 hours.

The current density, CD, may also influence the penetration depth due to its influence on the CR of the melt at the cathode surface. Sodium ions are the charge carriers in the electrolyte while Al-O-F complexes are discharged giving aluminium metal. With increasing CD the NaF concentration and hence the CR will increase in the melt on the cathode surface. Figure 4 shows the increased penetration depth with increasing CD for CR=4 reaching a plateau around 0.3 A/cm^2, again in good agreement with earlier experiments for pure carbon cathodes [16]. Increasing the current density further, the penetration depth increased, however, reaching a new plateau around 0.7 A/cm^2. This is probably connected to the presence of TiB_2 and better wetting conditions at the higher current density. Contrary to experiment with low current densities, a complete wetting of aluminium was observed at 1.0 A/cm^2 and the aluminium film adhered strongly to the cathode hindering the access of the electrolyte. This then demonstrates an advantage by using TiB_2 cathodes.

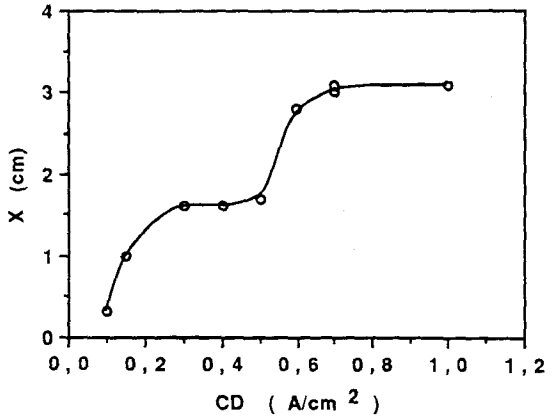

Figure 4. Plot of the sodium penetration depth versus the current density. T35 samples, CR=4, 1000°C, 4 hours.

3. Effect of TiB_2 Contents in Cathodes on Sodium Penetration Rate

For this part of the study, the electrolysis was performed at 0.5 A/cm^2 and 1000°C. The electrolyte contained 5 % Al_2O_3 and 5 % CaF_2 with a basic cryolite ratio (CR = 4). The test specimens were subjected to electrolysis, for 1, 2 and 4 hours, respectively.

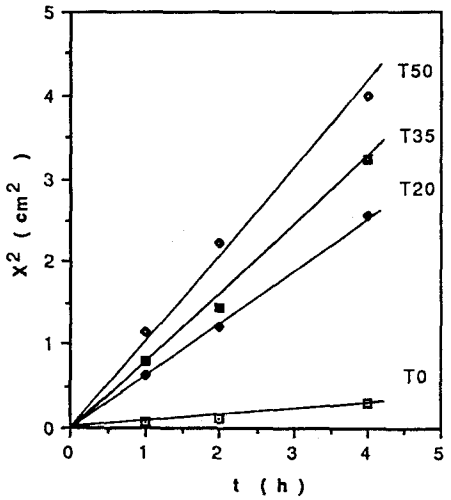

Figure 5. Plots of the square of sodium penetration depth versus time of electrolysis. CR = 4, CD = 0.5 A/cm^2, 1000°C.

The results can be understood by introducing Fick's second law. The cylindrical specimen is considered as an semi-infinite solid column and the supply source of sodium as an infinite reservoir, relative to the sufficiently short time of electrolysis. The assumed boundary conditions is that the concentration of sodium at the cathode surface (x = 0), C_s, and the concentration in the specimen at the beginning of diffusing (t = 0), C_o, are all constant during electrolysis. If the $C_{x,t}$ is the concentration at the diffusion depth x at time t, the solution to Fick's second law is below [20]:

$$\frac{C_{x,t} - C_o}{C_s - C_o} = \frac{1}{2}\left[1 - \mathrm{erf}\left(\frac{x}{2\sqrt{Dt}}\right)\right] \quad (4)$$

$$K = \frac{x}{2\sqrt{Dt}} \qquad (5)$$

At a constant $C_{x,t}$, the K is also constant. This gives a dynamic characterization for diffusion controlled process.

Figure 5 shows that the expected straight line $x^2 = bt$ is satisfied by most of the data obtained whether with or without TiB_2, and confirms the assumption of a diffusion controlled process. But the penetration in TiB_2-carbon cathodes was more rapid than that in pure carbon, and the velocity rose as the content of TiB_2 increased in the range of 20% - 50% TiB_2.

Table 3. Value of the constant b.

Sample type	b (cm^2/h)
T0	0.082
T20	0.638
T35	0.806
T50	0.994

The increased value of b (Table 3) implies that the doping of TiB_2 into carbon matrix has introduced some high diffusivity path in sodium diffusion mechanism [21] or some chemical potential relations forming a high surface concentration of sodium or both.

4. Distribution of Penetrated Sodium and Bath Constituents in TiB_2-Carbon Cathodes

The microprobe analysis was first made on a specimen as prepared, the photo in Figure 6 showing the central part of the T35 sample. The TiB_2 particles were dispersed over the carbon matrix, occupying about 1/3 part of the surface. Although this dispersion was far from being continuous over the entire cathode surface, the wetting of cryolite melts was still much better on the TiB_2-carbon cathodes than on the pure carbon, as observed in a study of contact angle [22].

Figure 6 also shows that TiB_2 particles bond well to the carbon matrix. Some pores existed in the carbon phase, but no evidence was found that they had a preference for the adjacent region around the TiB_2 particles. After a mechanical cutting, no cracks was observed along the interfacial region between TiB_2 and carbon, and only a few of the TiB_2 particles were broken in glasslike manner (Figure 6, right hand side bottom). In addition, x-ray emission of oxygen was made for checking the oxidation of TiB_2 or carbon during baking. Only a few signals of oxygen other than the background noise were found. This suggests that no significant oxidation or oxygen diffusion occurred in the interior of cathode specimens.

A T35 sample was subjected to electrolysis at 0.7 A/cm^2 for 4 hours (CR=4), and then a cut section was taken from 4 mm above the electrolyte level, assuming this area having been sufficiently penetrated by sodium and bath. A more detailed analysis was carried out in a TiB_2 and a carbon area, respectively. Figure 7 shows that a number of particles were inserted in the TiB_2 boundaries. From element x-ray dot maps of Na, Al and F, it is clear that the particles were formed by the penetrated bath constituents, mainly by NaF as most of the fluorine was located at the same sites as sodium. The salt particles appear to be separated without any strong bond to TiB_2 grains. Besides, metallic sodium migrated into the TiB_2 grains in a concentration lower than that on the boundaries while fluorine did not intrude into the grains. Aluminium impregnated the grains and boundaries without remarkable difference in concentration, and most of it was not combined with fluorine, possibly being present as metal in some alloys.

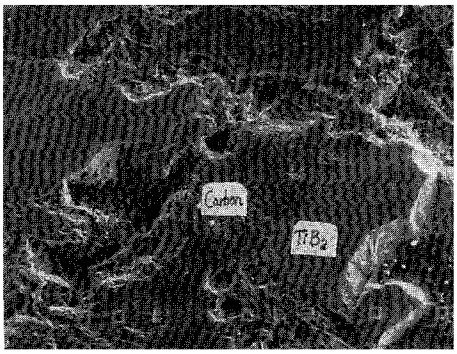

100 μm

Figure 6. Electron image of TiB_2-carbon cathode specimen as prepared.

Figure 8 shows that the particles of bath constituents were only occasionally found in the carbon area. The x-ray dot map demonstrates that sodium was present here in a higher concentration than that in TiB_2, yet it was scarcely accompanied with fluorine. This means that almost all the sodium was intercalated with the carbon matrix. Most of the Al was not present together with F, probably existing in the form of Al_4C_3.

Comparing Figures 7 and 8, it can be seen that the fluorides are less in the carbon area than in the TiB_2 area. This phenomenon may be interpreted as: TiB_2 particles are better wetted by molten fluorides of aluminium and sodium, and adsorb more easily fluorides from their surrounding area. In the carbon area, penetrated AlF_3 was depleted by the reaction below:

$$4\ Na_3AlF_6\ (l) + 12\ Na\ (\text{in C}) + 3\ C\ (s) = Al_4C_3\ (s) + 24\ NaF\ (l) \qquad (6)$$

Then the NaF-containing melt would preferentially migrate to the better wettable TiB_2. Moreover, the precipitation of NaF on the TiB_2 boundaries together with the presence of Al in the TiB_2 areas may reestablish reaction (3) inside the TiB_2-carbon cathode, thus increasing the sodium activity and possibly contributing to the increased Na penetration velocity.

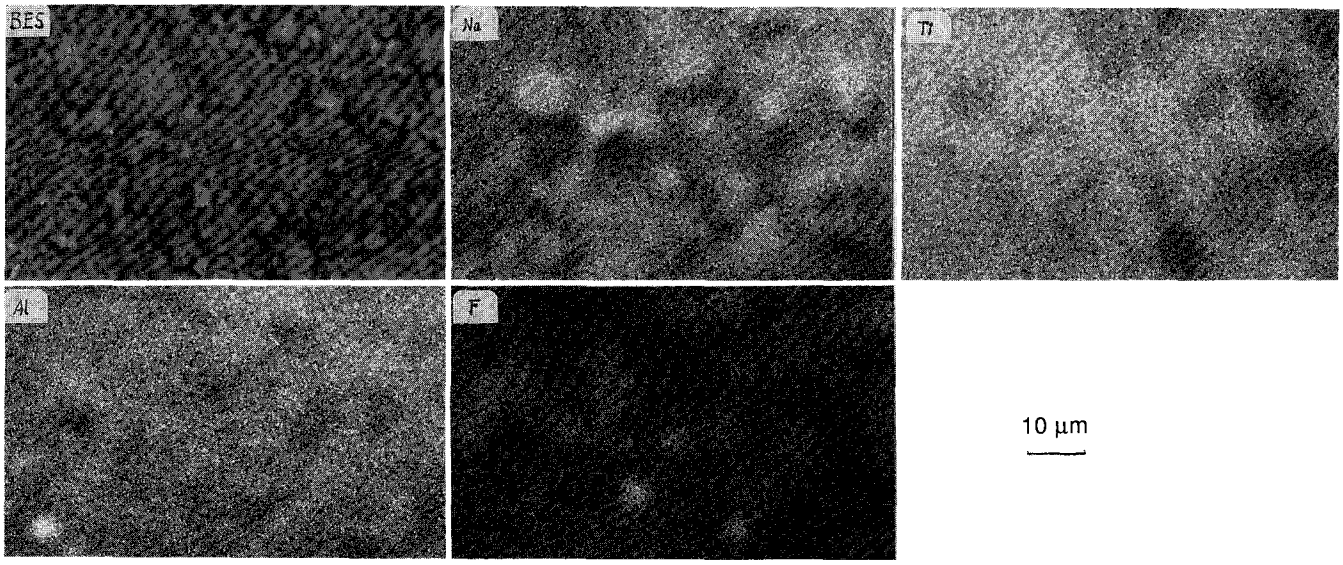

Figure 7. Electron microprobe analysis of the TiB_2 area of specimen after electrolysis.

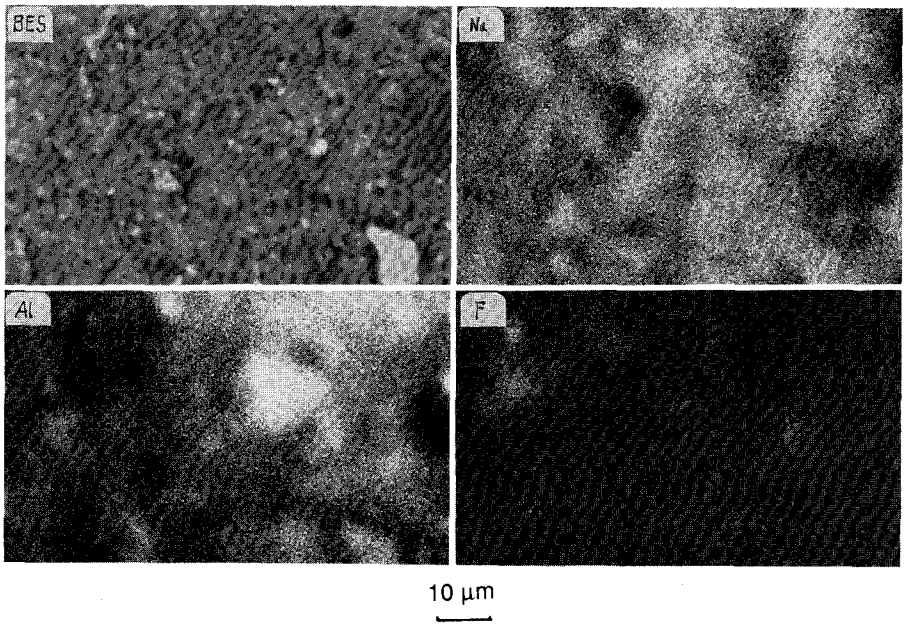

Figure 8. Electrone microprobe analysis of the carbon area of specimen after electrolysis.

CONCLUSIONS

1. TiB_2 was strongly bonded to carbon matrix by pressing and baking, giving this cathode increased crushing strength and decreased shrinkage during baking when the TiB_2 content varied by 20% - 50%.

2. Sodium penetration into TiB_2-carbon cathodes is a diffusion controlled process and its velocity increased as TiB_2 contents increased, as well as cryolite ratio and current density did, but reached a plateau at CR=3 or at 0.7 A/cm^2, respectively.

3. More fluorides of bath constituents were present on grain boundaries in TiB_2 areas, and more sodium was intercalated in carbon areas where AlF_3 was depleted, while NaF would preferentially migrate to the TiB_2 areas and enhance sodium generation and penetration.

ACKNOWLEDGEMENTS

The authors appreciate financial support from *The Royal Norwegian Council for Scientific and Industrial Research (NTNF)* and *The Norwegian Aluminium Industry.*

REFERENCES

1. K. Billehaug and H.A. Øye, "Inert Cathodes for Aluminium Electrolysis in Hall-Héroult Cells", **Aluminium**, 56 (1980), 642-648 and 713-718.

2. R.C. Dorward, "Energy Consumption of Aluminium Smelting Cells Containing Solid Wetted Cathodes", **J. Appl. Electrochem,** 1 (1983), 569-575.

3. B. Mazza, A. Bonfiglioli, F. Gregu and G. Serravalle, "Process Aspects in Aluminium Reduction Cells with Wettable Cathodes", **Aluminium**, 60 (1984), 760-763.

4. L.G. Boxall, A.V. Cooke and H.W. Hayden, "TiB_2 Cathode Material: Application in Conventional VSS Cells, **J. Met.**, 36 (1984), 35-40.

5. A.V. Cooke and W.M. Buchta, " Use of TiB_2 Cathode Material: Demonstrated Energy Conservation in VSS Cells", **Light Metals 1985**, H.O. Bohner, ed., Metallurgical Society of AIME, Warrendale, PA, 1985, 545-566.

6. K. Grjotheim, H. Kvande, Qiu Zhuxian and Xue Jilai, "Aluminium Electrolysis in a 100 A Laboratory Cell with Inert Electrodes", **Metall**, 42 (1988), 587-589.

7. R.P. Pawlek, "Cathodes Wettable by Molten Aluminium for Electrolysis Cells", **Aluminium,** 6 (1990), 573-581.

8. A.J. Gesing and D.J. Wheeler, "Screening and Evaluation Methods of Cathode Materials for Use in Aluminum Reduction Cells in Presence of Molten Aluminum and Cryolite up to 1000°C", **Light Metals 1987,** R.D. Zabreznik, ed., Metallurgical Society of AIME, Warrendale, PA, 1987, 327-333.

9. K.W. Tucker, J.T. Gee, J.R. Shaner, L.A. Joo', A.T. Tabereaux, D.V. Stewart and N.E. Richards, "Stable TiB_2 Graphite Cathodes for Aluminum Production", **Light Metals 1987**, R.D. Zabreznik, ed., Metallurgical Society of AIME, Warrendale, PA, 1987, 345-349.

10. T.R. Alcorn, D.V. Stewart, A.T. Tabereaux, L.A. Joo and K.W. Tucker, "Pilot Reduction Cell Operation Using TiB_2-G Cathodes", **Light Metals 1990**, Christian M. Bickert, ed., Metallurgical Society of AIME, Warrendale, PA, 1990, 413-418.

11. N.J. Finch, "The Mutual Solubilities of Titanium and Boron in Pure Aluminium", **Met. Trans.** 3 (1972), 2709-2711.

12. B. Mazza, G. Serravalle, G. Fumagalli and F. Brunella, "Cathode Behavior of Titanium Diboride in Aluminium Electrolysis", **J. Electrochem. Soc.**, 134 (1987), 1187-1191.

13. M.B. Dell, "Reaction Between Carbon Lining and Hall Bath", **Extractive Metallurgy of Aluminium,** Vol. 2, G. Gerard, ed., Interscience publishers, New York 1963, 403-415.

14. E.W. Dewing, "The Reaction of Sodium with Nongraphitic Carbon: Reactions Occurring in the Linings of Aluminum Reduction Cells", **Trans. Met. Soc. AIME** 22 (1963), 1328-1334.

15. C. Krohn, M. Sørlie and H. A. Øye, "Penetration of Sodium and Bath Constituents into Cathode Carbon Materials Used in Industrial Cells", **Light Metals 1982**, J.E. Andersen, ed., Metallurgical Society of AIME, Warrendale, PA, 1982, 311-324.

16. M. Sørlie and H. A. Øye, "Chemical Resistance of Cathode Carbon Materials during Electrolysis", **Light Metals 1984**, J.P. McGeer, ed., Metallurgical Society of AIME, Warrendale, PA, 1984, 1059-1070.

17. Xue Jilai and Qiu Zhuxian, "A Study of the Corrosion Resistance of the Electrodeposited TiB_2 Coating Cathode", **J. Northeast University of Technology,** 47 (1986), 33-37 (in Chinese). Ref.: C.A., 105.160883e.

18. DIN 51, 910, **"Bestimmung der Druckfestigkeit"**, 1981.

19. Morten Sørlie and Harald A. Øye, **Cathodes in Aluminium Electrolysis**, Aluminium-Verlag, Düsseldorf, Germany, 1989.

20. J. Crank, **Mathematics of Diffusion**, Oxford University Press, Fair Lawn, N. J.,1956.

21. Paul G. Shewmon, **Diffusion in Solids,** McGraw-Hill Company, New York, NY, 1962.

22. J. Xue and H.A. Øye, "Effect of TiB_2 in Carbon Matrix Cathode on the Wetting by Cryolite Melts and the Penetration of Sodium", Proceedings of the 42nd Meeting of ISE, Montreux, Switzerland, 1991, (7) 95.